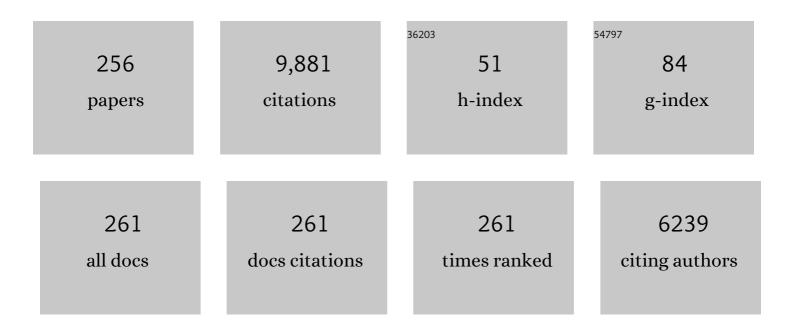


List of Publications by Year in descending order

Source: https://exaly.com/author-pdf/3224790/publications.pdf Version: 2024-02-01



YIANG CAO

#	Article	IF	CITATIONS
1	The activity and characterization of CeO2-TiO2 catalysts prepared by the sol–gel method for selective catalytic reduction of NO with NH3. Journal of Hazardous Materials, 2010, 174, 734-739.	6.5	411
2	Plasma-catalytic removal of formaldehyde over Cu–Ce catalysts in a dielectric barrier discharge reactor. Applied Catalysis B: Environmental, 2015, 170-171, 293-300.	10.8	270
3	Relationship between structure and performance of a novel cerium-niobium binary oxide catalyst for selective catalytic reduction of NO with NH3. Applied Catalysis B: Environmental, 2013, 142-143, 290-297.	10.8	255
4	Preparation and characterization of CeO2/TiO2 catalysts for selective catalytic reduction of NO with NH3. Catalysis Communications, 2010, 11, 465-469.	1.6	250
5	Recent Advances in Catalysts for Methane Combustion. Catalysis Surveys From Asia, 2015, 19, 140-171.	1.0	208
6	Tuning of catalytic sites in Pt/TiO2 catalysts for the chemoselective hydrogenation of 3-nitrostyrene. Nature Catalysis, 2019, 2, 873-881.	16.1	183
7	CO2 mineralization and utilization by alkaline solid wastes for potential carbon reduction. Nature Sustainability, 2020, 3, 399-405.	11.5	182
8	Hg ⁰ Capture over CoMoS/γ-Al ₂ O ₃ with MoS ₂ Nanosheets at Low Temperatures. Environmental Science & Technology, 2016, 50, 1056-1064.	4.6	157
9	Atmospheric Emission Characteristics and Control Policies of Five Precedent-Controlled Toxic Heavy Metals from Anthropogenic Sources in China. Environmental Science & Technology, 2015, 49, 1206-1214.	4.6	138
10	A Ce–Cu–Ti oxide catalyst for the selective catalytic reduction of NO with NH3. Catalysis Communications, 2010, 12, 255-258.	1.6	136
11	CeO ₂ –TiO ₂ Sorbents for the Removal of Elemental Mercury from Syngas. Environmental Science & Technology, 2013, 47, 10056-10062.	4.6	134
12	Non-Thermal Plasmas for VOCs Abatement. Plasma Chemistry and Plasma Processing, 2014, 34, 1033-1065.	1.1	130
13	Formation, transformation, measurement, and control of SO3 in coal-fired power plants. Fuel, 2019, 241, 327-346.	3.4	125
14	Post-plasma catalytic removal of methanol over Mn–Ce catalysts in an atmospheric dielectric barrier discharge. Applied Catalysis B: Environmental, 2016, 183, 124-132.	10.8	118
15	Enhanced performance for plasma-catalytic oxidation of ethyl acetate over La1-xCexCoO3+δ catalysts. Applied Catalysis B: Environmental, 2017, 213, 97-105.	10.8	116
16	Improvement in activity and alkali resistance of a novel V-Ce(SO4)2/Ti catalyst for selective catalytic reduction of NO with NH3. Applied Catalysis B: Environmental, 2017, 206, 449-460.	10.8	114
17	Granular bed filter: A promising technology for hot gas clean-up. Powder Technology, 2013, 244, 93-99.	2.1	113
18	Quantitative assessment of industrial VOC emissions in China: Historical trend, spatial distribution, uncertainties, and projection. Atmospheric Environment, 2017, 150, 116-125.	1.9	113

#	Article	IF	CITATIONS
19	Effects of PbCl2 on selective catalytic reduction of NO with NH3 over vanadia-based catalysts. Journal of Hazardous Materials, 2014, 274, 270-278.	6.5	110
20	Gas–liquid absorption reaction between (NH4)2SO3 solution and SO2 for ammonia-based wet flue gas desulfurization. Applied Energy, 2010, 87, 2647-2651.	5.1	109
21	A model for performance optimization of wet flue gas desulfurization systems of power plants. Fuel Processing Technology, 2008, 89, 1025-1032.	3.7	107
22	Structural defects in 2D MoS2 nanosheets and their roles in the adsorption of airborne elemental mercury. Journal of Hazardous Materials, 2019, 366, 240-249.	6.5	107
23	Investigation of the effect of Cu addition on the SO2-resistance of a CeTi oxide catalyst for selective catalytic reduction of NO with NH3. Fuel, 2012, 92, 49-55.	3.4	104
24	The co-effect of Sb and Nb on the SCR performance of the V2O5/TiO2 catalyst. Journal of Colloid and Interface Science, 2012, 368, 406-412.	5.0	102
25	New insights into the various decomposition and reactivity behaviors of NH4HSO4 with NO on V2O5/TiO2 catalyst surfaces. Chemical Engineering Journal, 2016, 283, 846-854.	6.6	101
26	The effect of ozone addition on combustion: Kinetics and dynamics. Progress in Energy and Combustion Science, 2019, 73, 1-25.	15.8	92
27	Physicochemical properties of metal-doped activated carbons and relationship with their performance in the removal of SO2 and NO. Journal of Hazardous Materials, 2011, 188, 58-66.	6.5	90
28	Deactivation mechanism of arsenic and resistance effect of SO42â^' on commercial catalysts for selective catalytic reduction of NO with NH3. Chemical Engineering Journal, 2016, 293, 118-128.	6.6	86
29	Investigation of hybrid plasma-catalytic removal of acetone over CuO/γ-Al 2 O 3 catalysts using response surface method. Chemosphere, 2016, 155, 9-17.	4.2	85
30	Mechanistic investigation of enhanced reactivity of NH4HSO4 and NO on Nb- and Sb-doped VW/Ti SCR catalysts. Applied Catalysis A: General, 2018, 549, 310-319.	2.2	84
31	Catalyst screening for acetone removal in a single-stage plasma-catalysis system. Catalysis Today, 2015, 256, 108-114.	2.2	80
32	Effect of H2S/HCl on the removal of elemental mercury in syngas over CeO2–TiO2. Chemical Engineering Journal, 2014, 241, 131-137.	6.6	78
33	Attractive Pickering Emulsion Gels. Advanced Materials, 2021, 33, e2102362.	11.1	78
34	On the Redox Mechanism of Lowâ€Temperature NH ₃ â€6CR over Cuâ€CHA: A Combined Experimental and Theoretical Study of the Reduction Half Cycle. Angewandte Chemie - International Edition, 2021, 60, 7197-7204.	7.2	77
35	Challenge of SO3 removal by wet electrostatic precipitator under simulated flue gas with high SO3 concentration. Fuel, 2018, 217, 597-604.	3.4	74
36	Comprehensive understanding of SO3 effects on synergies among air pollution control devices in ultra-low emission power plants burning high-sulfur coal. Journal of Cleaner Production, 2019, 239, 118096.	4.6	70

#	Article	IF	CITATIONS
37	Low temperature catalytic oxidation of propane over cobalt-cerium spinel oxides catalysts. Applied Surface Science, 2019, 479, 1132-1140.	3.1	70
38	Removal and Emission Characteristics of Condensable Particulate Matter in an Ultralow Emission Power Plant. Energy & Fuels, 2018, 32, 10586-10594.	2.5	66
39	Graphene-like MoS2 containing adsorbents for Hg0 capture at coal-fired power plants. Applied Energy, 2017, 207, 254-264.	5.1	64
40	Adsorption and reduction of NO2 over activated carbon at low temperature. Fuel Processing Technology, 2011, 92, 139-146.	3.7	63
41	Experimental study of acetone removal by packed-bed dielectric barrier discharge reactor. Journal of Industrial and Engineering Chemistry, 2014, 20, 2761-2768.	2.9	61
42	The Influence of Alkali Metals on the Ceâ€ī i Mixed Oxide Catalyst for the Selective Catalytic Reduction of NO _{<i>x</i>} . ChemCatChem, 2012, 4, 2075-2081.	1.8	59
43	MoO3-adjusted δ-MnO2 nanosheet for catalytic oxidation of Hg0 to Hg2+. Applied Catalysis B: Environmental, 2020, 263, 117829.	10.8	59
44	Simultaneous oxidation of NO, SO2 and Hg0 from flue gas by pulsed corona discharge. Journal of Environmental Sciences, 2009, 21, 328-332.	3.2	57
45	Nitrogen oxide absorption and nitrite/nitrate formation in limestone slurry for WFGD system. Applied Energy, 2014, 129, 187-194.	5.1	57
46	The Reaction of Poisonous Alkali Oxides with Vanadia SCR Catalyst and the Afterward Influence: A DFT and Experimental Study. Journal of Physical Chemistry C, 2015, 119, 1905-1912.	1.5	57
47	A combined wet electrostatic precipitator for efficiently eliminating fine particle penetration. Fuel Processing Technology, 2018, 180, 122-129.	3.7	57
48	Structure and crystal phase transition effect of Sn doping on anatase TiO2 for dichloromethane decomposition. Journal of Hazardous Materials, 2019, 371, 156-164.	6.5	57
49	Theoretical and experimental study on the deactivation of V2O5 based catalyst by lead for selective catalytic reduction of nitric oxides. Catalysis Today, 2011, 175, 625-630.	2.2	55
50	An experimental and modelling study of the reactivity of adsorbed NH3 in the low temperature NH3-SCR reduction half-cycle over a Cu-CHA catalyst. Applied Catalysis B: Environmental, 2020, 279, 119397.	10.8	55
51	An experimental study on the effects of temperature and pressure on negative corona discharge in high-temperature ESPs. Applied Energy, 2016, 164, 28-35.	5.1	54
52	Designing SO2-resistant cerium-based catalyst by modifying with Fe2O3 for the selective catalytic reduction of NO with NH3. Molecular Catalysis, 2019, 462, 10-18.	1.0	54
53	Preparation of Quaternized Bamboo Cellulose and Its Implication in Direct Air Capture of CO ₂ . Energy & Fuels, 2019, 33, 1745-1752.	2.5	54
54	Numerical simulation on the fine particle charging and transport behaviors in a wire-plate electrostatic precipitator. Advanced Powder Technology, 2016, 27, 1905-1911.	2.0	53

#	Article	IF	CITATIONS
55	Relationship between the molecular structure of V ₂ O ₅ /TiO ₂ catalysts and the reactivity of SO ₂ oxidation. Catalysis Science and Technology, 2016, 6, 1187-1194.	2.1	53
56	Particle migration and collection in a high-temperature electrostatic precipitator. Separation and Purification Technology, 2015, 143, 184-191.	3.9	52
57	Supported metal sulfates on Ce–TiOx as catalysts for NH3–SCR of NO: High resistances to SO2 and potassium. Journal of Industrial and Engineering Chemistry, 2016, 36, 271-278.	2.9	52
58	Effect of electrode configuration on particle collection in a high-temperature electrostatic precipitator. Separation and Purification Technology, 2016, 166, 157-163.	3.9	50
59	Microstructure and Mechanical Properties of High-Toughness Fiber-Reinforced Cementitious Composites after Exposure to Elevated Temperatures. Journal of Materials in Civil Engineering, 2016, 28, .	1.3	50
60	Partitioning of Hazardous Trace Elements among Air Pollution Control Devices in Ultra-Low-Emission Coal-Fired Power Plants. Energy & Fuels, 2017, 31, 6334-6344.	2.5	50
61	Identification of the reaction pathway and reactive species for the selective catalytic reduction of NO with NH ₃ over cerium–niobium oxide catalysts. Catalysis Science and Technology, 2016, 6, 2136-2142.	2.1	49
62	Electric agglomeration modes of coal-fired fly-ash particles with water droplet humidification. Fuel, 2017, 200, 134-145.	3.4	49
63	Numerical simulation of corona discharge and particle transport behavior with the particle space charge effect. Journal of Aerosol Science, 2018, 118, 22-33.	1.8	49
64	Plasma-catalytic removal of a low concentration of acetone in humid conditions. RSC Advances, 2014, 4, 37796-37805.	1.7	48
65	Experimental and theoretical studies on the influence of water vapor on the performance of a Ce-Cu-Ti oxide SCR catalyst. Applied Surface Science, 2013, 270, 370-376.	3.1	47
66	Investigation of the promotion effect of WO ₃ on the decomposition and reactivity of NH ₄ HSO ₄ with NO on V _{O₅–WO₃/TiO₂ SCR catalysts. RSC Advances, 2016, 6, 55584-55592.}	1.7	47
67	Life cycle assessment on biogas production from straw and its sensitivity analysis. Bioresource Technology, 2016, 201, 208-214.	4.8	47
68	Catalyst Design Based on DFT Calculations: Metal Oxide Catalysts for Gas Phase NO Reduction. Journal of Physical Chemistry C, 2014, 118, 13617-13622.	1.5	46
69	Plasma-catalytic decomposition of ethyl acetate over LaMO3 (M = Mn, Fe, and Co) perovskite catalysts. Journal of Industrial and Engineering Chemistry, 2019, 70, 447-452.	2.9	46
70	Synthesis and characterization of single-phase submicron zeolite Y from coal fly ash and its potential application for acetone adsorption. Microporous and Mesoporous Materials, 2020, 295, 109940.	2.2	46
71	Highly efficient removal of sulfuric acid aerosol by a combined wet electrostatic precipitator. RSC Advances, 2018, 8, 59-66.	1.7	44
72	Insights into the role of ionic wind in honeycomb electrostatic precipitators. Journal of Aerosol Science, 2019, 133, 83-95.	1.8	44

#	Article	IF	CITATIONS
73	Atmospheric emission inventory of SO3 from coal-fired power plants in China in the period 2009–2014. Atmospheric Environment, 2019, 197, 14-21.	1.9	43
74	Characteristics of negative DC corona discharge in a wire–plate configuration at high temperatures. Separation and Purification Technology, 2015, 139, 5-13.	3.9	42
75	Kinetics of NOxAbsorption into (NH4)2SO3Solution in an Ammonia-Based Wet Flue Gas Desulfurization Process. Energy & Fuels, 2010, 24, 5876-5882.	2.5	41
76	Numerical simulation of selective catalytic reduction of NO and SO2 oxidation in monolith catalyst. Chemical Engineering Journal, 2019, 361, 874-884.	6.6	41
77	Transient Kinetic Analysis of Low-Temperature NH ₃ -SCR over Cu-CHA Catalysts Reveals a Quadratic Dependence of Cu Reduction Rates on Cu ^{II} . ACS Catalysis, 2021, 11, 4821-4831.	5.5	41
78	Study on Catalytic Soot Oxidation over Spinel Type ACo2O4 (A = Co, Ni, Cu, Zn) Catalysts. Aerosol and Air Quality Research, 2017, 17, 2317-2327.	0.9	40
79	Numerical simulation of temperature effect on particles behavior via electrostatic precipitators. Applied Thermal Engineering, 2015, 88, 127-139.	3.0	39
80	Experimental investigation on charging characteristics and penetration efficiency of PM2.5 emitted from coal combustion enhanced by positive corona pulsed ESP. Journal of Electrostatics, 2009, 67, 799-806.	1.0	38
81	Experimental Study on Electrostatic Precipitation of Low-Resistivity High-Carbon Fly Ash at High Temperature. Energy & Fuels, 2017, 31, 6266-6273.	2.5	38
82	Assessment of winter air pollution episodes using long-range transport modeling in Hangzhou, China, during World Internet Conference, 2015. Environmental Pollution, 2018, 236, 550-561.	3.7	38
83	New insight into alkali resistance and low temperature activation on vanadia-titania catalysts for selective catalytic reduction of NO. Applied Surface Science, 2019, 466, 99-109.	3.1	38
84	Synthesis, characterization and catalytic performances of Cu- and Mn-containing ordered mesoporous carbons for the selective catalytic reduction of NO with NH ₃ . Catalysis Science and Technology, 2015, 5, 1267-1279.	2.1	37
85	Controllable synthesis of hierarchical MnO x /TiO 2 composite nanofibers for complete oxidation of low-concentration acetone. Journal of Hazardous Materials, 2017, 337, 105-114.	6.5	37
86	Experimental study on the evaporation and chlorine migration of desulfurization wastewater in flue gas. Environmental Science and Pollution Research, 2019, 26, 4791-4800.	2.7	37
87	Experimental study on the removal of SO3 from coal-fired flue gas by alkaline sorbent. Fuel, 2020, 259, 116306.	3.4	37
88	Simulation of SO2 absorption and performance enhancement of wet flue gas desulfurization system. Chemical Engineering Research and Design, 2021, 150, 453-463.	2.7	37
89	Unraveling the Hydrolysis of Z ₂ Cu ²⁺ to ZCu ²⁺ (OH) ^{â^'} and Its Consequences for the Low-Temperature Selective Catalytic Reduction of NO on Cu-CHA Catalysts. ACS Catalysis, 2021, 11, 11616-11625.	5.5	37
90	Bimetallic cerium–copper nanoparticles embedded in ordered mesoporous carbons as effective catalysts for the selective catalytic reduction of NO with NH3. Journal of Colloid and Interface Science, 2015, 456, 66-75.	5.0	36

#	Article	IF	CITATIONS
91	Synthesis and characterization of a single phase zeolite A using coal fly ash. RSC Advances, 2018, 8, 42200-42209.	1.7	36
92	KOH-activated hydrochar with engineered porosity as sustainable adsorbent for volatile organic compounds. Colloids and Surfaces A: Physicochemical and Engineering Aspects, 2020, 588, 124372.	2.3	36
93	Fine particle migration and collection in a wet electrostatic precipitator. Journal of the Air and Waste Management Association, 2017, 67, 498-506.	0.9	35
94	Chemical characteristics and sources of PM1 during the 2016 summer in Hangzhou. Environmental Pollution, 2018, 232, 42-54.	3.7	35
95	Meteorological and chemical impacts on PM2.5 during a haze episode in a heavily polluted basin city of eastern China. Environmental Pollution, 2019, 250, 520-529.	3.7	35
96	Promotional effect of doping Cu into cerium-titanium binary oxides catalyst for deep oxidation of gaseous dichloromethane. Chemosphere, 2019, 214, 553-562.	4.2	35
97	Experimental investigation on the characteristics of ash layers in a high-temperature wire–cylinder electrostatic precipitator. Separation and Purification Technology, 2016, 159, 135-146.	3.9	34
98	La0.8M0.2MnO3 (M = Ba, Ca, Ce, Mg and Sr) perovskite catalysts for plasma-catalytic oxidation of ethyl acetate. Catalysis Communications, 2017, 92, 35-39.	1.6	34
99	Evolution of Condensable Fine Particle Size Distribution in Simulated Flue Gas by External Regulation for Growth Enhancement. Environmental Science & Technology, 2020, 54, 3840-3848.	4.6	34
100	Optimizing magnetic functionalization conditions for efficient preparation of magnetic biochar and adsorption of Pb(II) from aqueous solution. Science of the Total Environment, 2022, 806, 151442.	3.9	33
101	Removal of NOx with radical injection caused by corona discharge. Fuel, 2004, 83, 1349-1355.	3.4	32
102	Naphthalene decomposition in a DC corona radical shower discharge. Journal of Zhejiang University: Science A, 2011, 12, 71-77.	1.3	32
103	Numerical simulation of particle migration in electrostatic precipitator with different electrode configurations. Powder Technology, 2020, 361, 238-247.	2.1	32
104	An experimental investigation of electrostatic precipitation in a wire–cylinder configuration at high temperatures. Powder Technology, 2015, 269, 166-177.	2.1	31
105	Smog chamber study of the role of NH3 in new particle formation from photo-oxidation of aromatic hydrocarbons. Science of the Total Environment, 2018, 619-620, 927-937.	3.9	31
106	Insight into the significant roles of microstructures and functional groups on carbonaceous surfaces for acetone adsorption. RSC Advances, 2018, 8, 21541-21550.	1.7	31
107	Modeling and optimization of wet flue gas desulfurization system based on a hybrid modeling method. Journal of the Air and Waste Management Association, 2019, 69, 565-575.	0.9	31
108	Hg0-temperature-programmed surface reaction and its application on the investigation of metal oxides for Hg0 capture. Fuel, 2016, 181, 1089-1094.	3.4	30

#	Article	IF	CITATIONS
109	Synergy of vanadia and ceria in the reaction mechanism of low-temperature selective catalytic reduction of NOx by NH3. Journal of Catalysis, 2020, 391, 145-154.	3.1	30
110	Low temperature selective catalytic reduction of NO and NO2 with NH3 over activated carbon-supported vanadium oxide catalyst. Catalysis Today, 2011, 175, 164-170.	2.2	29
111	Adsorption of NO on ordered mesoporous carbon and its improvement by cerium. RSC Advances, 2014, 4, 16281.	1.7	29
112	Molecular Transformations of Arsenic Species in the Flue Gas of Typical Power Plants: A Density Functional Theory Study. Energy & Fuels, 2016, 30, 4209-4214.	2.5	29
113	Integrated Dynamic and Steady State Method and Its Application on the Screening of MoS ₂ Nanosheet-Containing Adsorbents for Hg ⁰ Capture. Energy & Fuels, 2018, 32, 5338-5344.	2.5	29
114	Insights into the role of particle space charge effects in particle precipitation processes in electrostatic precipitator. Powder Technology, 2018, 339, 606-614.	2.1	29
115	Characteristics and Uncertainty of Industrial VOCs Emissions in China. Aerosol and Air Quality Research, 2015, 15, 1045-1058.	0.9	29
116	Experimental Study on Removal Characteristics of SO ₃ by Wet Flue Gas Desulfurization Absorber. Energy & Fuels, 2018, 32, 6031-6038.	2.5	28
117	Cost estimate of the multi-pollutant abatement in coal-fired power sector in China. Energy, 2018, 161, 523-535.	4.5	28
118	Particle removal enhancement in a high-temperature electrostatic precipitator for glass furnace. Powder Technology, 2017, 319, 154-162.	2.1	27
119	Predicting particle collection performance of a wet electrostatic precipitator under varied conditions with artificial neural networks. Powder Technology, 2021, 377, 632-639.	2.1	27
120	Removal of NOx from wet flue gas by corona discharge. Fuel, 2004, 83, 1251-1255.	3.4	26
121	Characteristics of DC discharge in a wire-cylinder configuration at high ambient temperatures. Journal of Electrostatics, 2014, 72, 13-21.	1.0	26
122	Promotion effect of KOH surface etching on sucrose-based hydrochar for acetone adsorption. Applied Surface Science, 2019, 496, 143617.	3.1	26
123	Controllable synthesis of novel hierarchical V ₂ O ₅ /TiO ₂ nanofibers with improved acetone oxidation performance. RSC Advances, 2015, 5, 30416-30424.	1.7	25
124	Electrospinning synthesis of vanadium–TiO2–carbon composite nanofibrous membranes as effective catalysts for the complete oxidation of low-concentration acetone. Applied Catalysis A: General, 2015, 507, 99-108.	2.2	25
125	Manganese-cerium oxide catalysts prepared by non-thermal plasma for NO oxidation: Effect of O 2 in discharge atmosphere. Applied Surface Science, 2017, 416, 78-85.	3.1	25
126	Microwave-induced activation of additional active edge sites on the MoS 2 surface for enhanced Hg 0 capture. Applied Surface Science, 2017, 420, 439-445.	3.1	25

#	Article	IF	CITATIONS
127	Speciation Characteristics and Mobility of Trace Elements Across Ultralow Emission Air Pollution Control Devices. Energy & Fuels, 2017, 31, 13963-13971.	2.5	25
128	Effect of dust layer in electrostatic precipitators on discharge characteristics and particle removal. Fuel, 2020, 278, 118335.	3.4	25
129	Adsorption kinetics of NO on ordered mesoporous carbon (OMC) and cerium-containing OMC (Ce-OMC). Applied Surface Science, 2014, 317, 26-34.	3.1	24
130	Developments in Unipolar Charging of Airborne Particles: Theories, Simulations and Measurements. Aerosol and Air Quality Research, 2016, 16, 3037-3054.	0.9	24
131	Elemental Mercury Capture from Syngas by Novel High-Temperature Sorbent Based on Pd–Ce Binary Metal Oxides. Industrial & Engineering Chemistry Research, 2015, 54, 3678-3684.	1.8	23
132	Development of back corona discharge in a wire-cylinder electrostatic precipitator at high temperatures. Powder Technology, 2015, 286, 789-797.	2.1	23
133	Sulfuric Acid Aerosol Formation and Collection by Corona Discharge in a Wet Electrostatic Precipitator. Energy & amp; Fuels, 2017, 31, 8400-8406.	2.5	23
134	Different reactive behaviours of dichloromethane over anatase TiO2 supported RuO2 and V2O5. Catalysis Today, 2020, 355, 349-357.	2.2	23
135	Fast Evolution of Sulfuric Acid Aerosol Activated by External Fields for Enhanced Emission Control. Environmental Science & Technology, 2020, 54, 3022-3031.	4.6	23
136	Effect of multi-pollutant on the catalytic oxidation of dichloromethane over RuO2-WO3/Sn0.2Ti0.8O2 catalyst. Fuel, 2020, 278, 118207.	3.4	22
137	Exploring the role of V ₂ O ₅ in the reactivity of NH ₄ HSO ₄ with NO on V ₂ O ₅ /TiO ₂ SCR catalysts. RSC Advances, 2016, 6, 102436-102443.	1.7	21
138	Promotional effect of TiO2 on quinoline hydrodenitrogenation activity over Pt/γ-Al2O3 catalysts. Chemical Engineering Science, 2019, 207, 1085-1095.	1.9	21
139	Improvement of fuel sources and energy products flexibility in coal power plants via energy-cyber-physical-systems approach. Applied Energy, 2019, 254, 113554.	5.1	21
140	Integration of machine learning approaches for accelerated discovery of transition-metal dichalcogenides as HgO sensing materials. Applied Energy, 2019, 254, 113651.	5.1	21
141	Effect of KCl on the selective catalytic reduction of NO with NH ₃ over vanadiaâ€based catalysts for biomass combustion. Environmental Progress and Sustainable Energy, 2014, 33, 390-395.	1.3	20
142	CFD simulation of high-temperature effect on EHD characteristics in a wire-plate electrostatic precipitator. Chinese Journal of Chemical Engineering, 2015, 23, 633-640.	1.7	20
143	Development and Experimental Evaluation of a Continuous Monitor for SO ₃ Measurement. Energy & Fuels, 2017, 31, 9684-9692.	2.5	20
144	Measurement and prediction of fly ash resistivity over a wide range of temperature. Fuel, 2018, 216, 673-680.	3.4	20

#	Article	IF	CITATIONS
145	Balance and stability between particle collection and re-entrainment inawide temperature-range electrostatic precipitator. Powder Technology, 2018, 340, 543-552.	2.1	20
146	Evaporation and concentration of desulfurization wastewater with waste heat from coal-fired power plants. Environmental Science and Pollution Research, 2019, 26, 27494-27504.	2.7	20
147	Study of the Promotion Effect of Iron on Supported Manganese Catalysts for NO Oxidation. Aerosol and Air Quality Research, 2014, 14, 1038-1046.	0.9	20
148	Accelerated identification of high-performance catalysts for low-temperature NH ₃ -SCR by machine learning. Journal of Materials Chemistry A, 2021, 9, 23850-23859.	5.2	19
149	Dynamic Binuclear Cu ^{II} Sites in the Reduction Half-Cycle of Low-Temperature NH ₃ –SCR over Cu-CHA Catalysts. ACS Catalysis, 2022, 12, 5263-5274.	5.5	19
150	A DFT study on the behavior of NO2 in the selective catalytic reduction of nitric oxides with ammonia on a V2O5 catalyst surface. Journal of Molecular Catalysis A, 2010, 317, 46-53.	4.8	18
151	Effect of gas–liquid phase compositions on NO2 and NO absorption into ammonium-sulfite and bisulfite solutions. Fuel Processing Technology, 2011, 92, 1506-1512.	3.7	18
152	Catalytic oxidation of acetone over CuCeO _x nanofibers prepared by an electrospinning method. RSC Advances, 2014, 4, 43874-43881.	1.7	18
153	Investigating the role of H4SiW12O40 in the acidity, oxidability and activity of H4SiW12O40-Fe2O3 catalysts for the selective catalytic reduction of NO with NH3. Molecular Catalysis, 2018, 448, 177-184.	1.0	18
154	New Insights into the Decomposition Behavior of NH ₄ HSO ₄ on the SiO ₂ -Decorated SCR Catalyst and Its Enhanced SO ₂ -Resistant Ability. ACS Omega, 2019, 4, 4927-4935.	1.6	18
155	Systematic Approach to Optimization of Submicron Particle Agglomeration Using Ionic-Wind-Assisted Pre-Charger. Aerosol and Air Quality Research, 2015, 15, 2709-2719.	0.9	18
156	A Numerical Investigation of the Effect of Dust Layer on Particle Migration in an Electrostatic Precipitator. Aerosol and Air Quality Research, 2020, 20, 166-179.	0.9	18
157	Absorption of NO2 into Na2S solution in a stirred tank reactor. Journal of Zhejiang University: Science A, 2009, 10, 434-438.	1.3	17
158	Elemental mercury removal from syngas by nano-ZnO sorbent. Journal of Fuel Chemistry and Technology, 2013, 41, 1371-1377.	0.9	17
159	Mechanistic investigation of NH3 oxidation over V-0.5Ce(SO4)2/Ti NH3-SCR catalyst. Catalysis Communications, 2018, 112, 1-4.	1.6	17
160	Current density distribution and optimization of the collection electrodes of a honeycomb wet electrostatic precipitator. RSC Advances, 2018, 8, 30701-30711.	1.7	17
161	Field test of SO3 removal in ultra-low emission coal-fired power plants. Environmental Science and Pollution Research, 2020, 27, 4746-4755.	2.7	17
162	Numerical simulation of the simultaneous removal of particulate matter in a wet flue gas desulfurization system. Environmental Science and Pollution Research, 2020, 27, 1598-1607.	2.7	17

#	Article	IF	CITATIONS
163	Plasma-induced adsorption of elemental mercury on TiO 2 supported metal oxide catalyst at low temperatures. Fuel Processing Technology, 2015, 138, 14-20.	3.7	16
164	Experimental study on electrostatic removal of high-carbon particle in high temperature coal pyrolysis gas. Proceedings of the Combustion Institute, 2019, 37, 2959-2965.	2.4	16
165	Mechanism of Hg ⁰ and O ₂ Interaction on the IrO ₂ (110) Surface: A Density Functional Theory Study. Energy & Fuels, 2019, 33, 1354-1362.	2.5	16
166	Catalytic oxidation of Hg0 with O2 induced by synergistic coupling of CeO2 and MoO3. Journal of Hazardous Materials, 2020, 381, 121037.	6.5	16
167	Intrinsically Anisotropic Dielectric Elastomer Fiber Actuators. , 2022, 4, 472-479.		16
168	In-Situ Characterization of Coal Particle Combustion via Long Working Distance Digital In-Line Holography. Energy & Fuels, 2018, 32, 8277-8286.	2.5	15
169	On the Redox Mechanism of Lowâ€Temperature NH ₃ â€SCR over Cuâ€CHA: A Combined Experimental and Theoretical Study of the Reduction Half Cycle. Angewandte Chemie, 2021, 133, 7273-7280.	1.6	15
170	An integrated LSTM-AM and SPRT method for fault early detection of forced-oxidation system in wet flue gas desulfurization. Chemical Engineering Research and Design, 2022, 160, 242-254.	2.7	15
171	Co-benefit of hazardous trace elements capture in dust removal devices of ultra-low emission coal-fired power plants. Journal of Zhejiang University: Science A, 2018, 19, 68-79.	1.3	14
172	Supported Bimetallic AuPd Nanoparticles as a Catalyst for the Selective Hydrogenation of Nitroarenes. Nanomaterials, 2018, 8, 690.	1.9	14
173	Investigation on optimal active layer thickness and pore size in dual-layer NH3-SCR monolith for low SO2 oxidation by numerical simulation. Fuel, 2020, 279, 118420.	3.4	14
174	CFD simulation with enhancement factor of sulfur dioxide absorption in the spray scrubber. Journal of Zhejiang University: Science A, 2008, 9, 1601-1613.	1.3	13
175	Study of Geometry Structure on a Wire–Plate Pulsed Corona Discharge Reactor. IEEE Transactions on Plasma Science, 2012, 40, 802-810.	0.6	13
176	Experimental study of NO2 reduction in N2/Ar and O2/Ar mixtures by pulsed corona discharge. Journal of Environmental Sciences, 2014, 26, 2249-2256.	3.2	13
177	Enhanced particle precipitation from flue gas containing ultrafine particles through precharging. Chemical Engineering Research and Design, 2020, 144, 111-122.	2.7	13
178	Improving the removal of particles via electrostatic precipitator by optimizing the corona wire arrangement. Powder Technology, 2021, 388, 201-211.	2.1	13
179	Analysis on Leaching Characteristics of Iron in Coal Fly Ash under Ammonia-Based Wet Flue Gas Desulfurization (WFGD) Conditions. Energy & Fuels, 2009, 23, 5916-5919.	2.5	12
180	An analytical method for DC negative corona discharge in a wire-cylinder device at high temperatures. Journal of Electrostatics, 2014, 72, 270-284.	1.0	12

#	Article	IF	CITATIONS
181	Coupling Nonthermal Plasma with V ₂ O ₅ /TiO ₂ Nanofiber Catalysts for Enhanced Oxidation of Ethyl Acetate. Industrial & Engineering Chemistry Research, 2019, 58, 2-10.	1.8	12
182	The Effect of Cr Addition on Hg0 Oxidation and NO Reduction over V2O5/TiO2 Catalyst. Aerosol and Air Quality Research, 2018, 18, 803-810.	0.9	12
183	PbCl ₂ â€poisoning kinetics of V ₂ O ₅ /TiO ₂ catalysts for the selective catalytic reduction of NO with NH ₃ . Environmental Progress and Sustainable Energy, 2015, 34, 1085-1091.	1.3	11
184	Measurement of slurry droplets in coal-fired flue gas after WFGD. Environmental Geochemistry and Health, 2015, 37, 915-929.	1.8	11
185	A novel method of microwave heating mixed liquid-assisted regeneration of V2O5–WO3/TiO2 commercial SCR catalysts. Environmental Geochemistry and Health, 2015, 37, 905-914.	1.8	11
186	Promotional effects of ruthenium oxide on catalytic oxidation of dichloromethane over the tungsten-titanium binary oxides catalyst. Proceedings of the Combustion Institute, 2021, 38, 6461-6471.	2.4	11
187	Mechanism and Enhancement of the Low-Temperature Selective Catalytic Reduction of NO <i>x</i> with NH ₃ by Bifunctional Catalytic Mixtures. Industrial & Engineering Chemistry Research, 2021, 60, 6446-6454.	1.8	11
188	PLIF diagnostics of NO oxidization and OH consumption in pulsed corona discharge. Fuel, 2012, 102, 729-736.	3.4	10
189	Density functional theory study of the adsorption of elemental mercury on a 1T-MoS2 monolayer. Journal of Zhejiang University: Science A, 2018, 19, 60-67.	1.3	10
190	Speciation and Thermal Stability of Mercury in Solid Products from Ultralow Emission Air Pollution Control Devices. Energy & amp; Fuels, 2018, 32, 12655-12664.	2.5	10
191	Investigation of Arsenic Poisoned Selective Catalytic Reduction Catalyst Performance and Lifetime in Coal-Fired Power Plants. Energy & Fuels, 2020, 34, 12833-12840.	2.5	10
192	New insights into catalytic pyrolysis mechanisms and reaction pathways of urea pyrolysis on V–Ti catalyst surfaces. RSC Advances, 2016, 6, 108000-108009.	1.7	9
193	Experimental study on ZnO-TiO2 sorbents for the removal of elemental mercury. Korean Journal of Chemical Engineering, 2017, 34, 2383-2389.	1.2	9
194	Performance Analysis and Evaluation of a Supercritical CO2 Rankine Cycle Coupled with an Absorption Refrigeration Cycle. Journal of Thermal Science, 2020, 29, 1036-1052.	0.9	9
195	Particle capture in a high-temperature electrostatic precipitator with different electrode configurations. Powder Technology, 2020, 372, 84-93.	2.1	9
196	Hybrid Gas Sensor Array to Identify and Quantify Low-Concentration VOCs Mixtures Commonly Found in Chemical Industrial Parks. IEEE Sensors Journal, 2022, 22, 13434-13441.	2.4	9
197	Multi-Objective Load Dispatch Control of Biomass Heat and Power Cogeneration Based on Economic Model Predictive Control. Energies, 2021, 14, 762.	1.6	8
198	Experiments on Enhancing the Particle Charging Performance of an Electrostatic Precipitator. Aerosol and Air Quality Research, 2019, 19, 1411-1420.	0.9	8

#	Article	IF	CITATIONS
199	Desulfurization Characteristic of Calcium-Based Sorbent during Activation Process Journal of Chemical Engineering of Japan, 2001, 34, 1114-1119.	0.3	7
200	Planar Laser-Induced Fluorescence Diagnostics for Spatiotemporal OH Evolution in Pulsed Corona Discharge. IEEE Transactions on Plasma Science, 2013, 41, 485-493.	0.6	7
201	Simultaneous absorption of NOx and SO ₂ in oxidantâ€enhanced limestone slurry. Environmental Progress and Sustainable Energy, 2014, 33, 1171-1179.	1.3	7
202	Hybrid modeling scheme for PM concentration prediction of electrostatic precipitators. Powder Technology, 2018, 340, 163-172.	2.1	7
203	Energy consumption and energy-saving potential analysis of pollutant abatement systems in a 1000-MW coal-fired power plant. Journal of the Air and Waste Management Association, 2018, 68, 920-930.	0.9	7
204	Highly efficient recovery of molybdenum from spent catalyst by an optimized process. Journal of the Air and Waste Management Association, 2020, 70, 971-979.	0.9	7
205	Exploring the role of sulfuric acid aerosol in corona discharge through a honeycomb wet electrostatic precipitator. Chemical Engineering Research and Design, 2021, 146, 763-769.	2.7	7
206	Effect of Gas Components and Particulate Matter on the Conversion of Nitric Oxide by Dielectric Barrier Discharge. Energy & Fuels, 2021, 35, 6711-6724.	2.5	7
207	Dynamic NOx emission prediction based on composite models adapt to different operating conditions of coal-fired utility boilers. Environmental Science and Pollution Research, 2022, 29, 13541-13554.	2.7	7
208	Energy Consumption Analysis and OH Radical Detection of NO Conversion Process From Flue Gas Using Pulsed Corona Discharge. IEEE Transactions on Plasma Science, 2014, 42, 105-113.	0.6	6
209	Kinetic Studies on NO ₂ Absorption into Ammonium Sulfite Solutions. Separation Science and Technology, 2015, 50, 1433-1438.	1.3	6
210	Experimental investigation of sulfite oxidation enhancement in a micro-pore aeration system. RSC Advances, 2016, 6, 104139-104147.	1.7	6
211	A perspective on the applications of energy-cyber-physical systems (e-CPSs) in ultra-low emission coal-fired power plants. Energy Procedia, 2019, 158, 6139-6144.	1.8	6
212	An Amended Chemical Mass Balance Model for Source Apportionment of PM _{2.5} in Typical Chinese Eastern Coastal Cities. Clean - Soil, Air, Water, 2019, 47, 1800115.	0.7	6
213	Measurement techniques for sulfur trioxide concentration in coal-fired flue gas: a review. Environmental Science and Pollution Research, 2021, 28, 22278-22295.	2.7	6
214	A Probe into the Low-Temperature SCR Activity: NO Oxidative Activation to Nitrite-Intermediates. Catalysis Letters, 2022, 152, 1140-1144.	1.4	6
215	Investigation of the growth and removal of particles in coal-fired flue gas by temperature management. Fuel, 2021, 302, 121220.	3.4	6
216	Enhanced performance of Nb2O5 decorated RuO2/Sn0.2Ti0.8O2 for selective catalytic oxidation of ammonia. Chemical Engineering Research and Design, 2022, 160, 948-957.	2.7	6

#	Article	IF	CITATIONS
217	Environmental consequences of an ultra-low emission retrofit in coal-fired power plants from a life cycle perspective. Waste Disposal & Sustainable Energy, 2021, 3, 309-323.	1.1	6
218	An industrial demonstration study on CO2 mineralization curing for concrete. IScience, 2022, 25, 104261.	1.9	6
219	Air pollution control for a green future. Journal of Zhejiang University: Science A, 2018, 19, 1-4.	1.3	5
220	A Comparative Study of the NH3-SCR Reactions over an Original and Sb-Modified V2O5–WO3/TiO2 Catalyst at Low Temperatures. Energies, 2018, 11, 3339.	1.6	5
221	Molecular insights into the hydrodenitrogenation mechanism of pyridine over Pt/γ-Al2O3 catalysts. Molecular Catalysis, 2020, 495, 111148.	1.0	5
222	The relationship of morphology and catalytic performance of CeO2 catalysts for reducing nitrobenzene to azoxybenzene under the base-free condition. Chinese Chemical Letters, 2021, 32, 761-764.	4.8	5
223	Minimizing the adverse effects of dust layer on the particle migration in electrostatic precipitator under various temperature. Fuel Processing Technology, 2021, 213, 106659.	3.7	5
224	Whole life cycle performance evolution of selective catalytic reduction catalyst in coal-fired power plants. Fuel Processing Technology, 2021, 219, 106866.	3.7	5
225	Highly efficient selective extraction of Mo with novel hydrophobic deep eutectic solvents. Journal of the Air and Waste Management Association, 2021, 71, 1492-1501.	0.9	5
226	Density functional theory studies on ortho-position adsorption of SO3 at step sites of a CaO surface with SO2 and CO2. Fuel, 2022, 310, 122174.	3.4	5
227	Unexpected rise of atmospheric secondary aerosols from biomass burning during the COVID-19 lockdown period in Hangzhou, China. Atmospheric Environment, 2022, 278, 119076.	1.9	5
228	Co-Benefits of Pollutant Removal, Water, and Heat Recovery from Flue Gas through Phase Transition Enhanced by Corona Discharge. Environmental Science & Technology, 2022, 56, 8844-8853.	4.6	5
229	Catalytic Oxidation of Dimethyl Sulfide Over Commercial V-W/Ti Catalysts: Plasma Activation at Low Temperatures. IEEE Transactions on Plasma Science, 2016, 44, 3379-3385.	0.6	4
230	Enhancing PM Removal by Pulse Energized Electrostatic Precipitators—a Comparative Study. IEEE Transactions on Plasma Science, 2019, 47, 365-375.	0.6	4
231	Design and development of an ammonia slip detection device and system for flue gas denitration equipment. Chemical Engineering Research and Design, 2021, 153, 130-138.	2.7	4
232	Nonferrous metal flue gas purification based on high-temperature electrostatic precipitation. Chemical Engineering Research and Design, 2021, 154, 202-210.	2.7	4
233	Simulation of SO2 removal process from marine exhaust gas by hybrid exhaust gas cleaning systems (ECCS) using seawater and magnesium-based absorbent. Separation and Purification Technology, 2022, 287, 120557.	3.9	4
234	Effect of relative humidity on non-refractory submicron aerosol evolution during summertime in Hangzhou, China. Journal of Zhejiang University: Science A, 2018, 19, 45-59.	1.3	3

#	Article	IF	CITATIONS
235	Adopting Big Data to Accelerate Discovery of 2D TMDCs Materials via CVR Method for the Potential Application in Urban Airborne Hg0 Sensor. Energy Procedia, 2018, 152, 847-852.	1.8	3
236	Non-Thermal Plasma-Modified Ru-Sn-Ti Catalyst for Chlorinated Volatile Organic Compound Degradation. Catalysts, 2020, 10, 1456.	1.6	3
237	Simulation investigation on marine exhaust gas SO ₂ absorption by seawater scrubbing. Journal of the Air and Waste Management Association, 2022, 72, 383-402.	0.9	3
238	Detection of OH Radicals Generated in Wire–Plate Pulsed Corona Discharge by LIF. IEEE Transactions on Plasma Science, 2015, 43, 1747-1757.	0.6	2
239	Low-temperature electrostatic precipitator with different electrode configurations under various operation conditions. Powder Technology, 2021, 394, 1178-1185.	2.1	2
240	A002 DEVELOPMENT OF MULTI-POLLUTANTS CONTROL TECHNOLOGY FOR FLUE GAS FROM POWER PLANTS IN CHINA(Plenary Lecture). The Proceedings of the International Conference on Power Engineering (ICOPE), 2009, 2009.1, _1-91-14	0.0	2
241	The effect of transition metals (Me: Mn, Cu) on Pt/CeO2/Al2O3 catalysts for the catalytic reduction of NO by CO. Reaction Kinetics, Mechanisms and Catalysis, 2022, 135, 1553-1571.	0.8	2
242	Regeneration mechanism of CeO2-TiO2 sorbents for elemental mercury capture from syngas. Korean Journal of Chemical Engineering, 2016, 33, 1008-1013.	1.2	1
243	Particle charging in electric field under simulated SO3-containing flue gas at low temperature. Fuel, 2022, 310, 122291.	3.4	1
244	Removal of NO x by radical injection. Science Bulletin, 2004, 49, 1991-1995.	1.7	0
245	Simultaneous removal of SO <inf>2</inf> and NO from coal flue gas with NaClO <inf>2</inf> / KMnO <inf>4</inf> enhanced Ca-based sorbent. , 2011, , .		0
246	Experimental study on combined deactivating effect of K and Ca on SCR catalysts. , 2011, , .		0
247	Numerical investigation of the effect of particle concentration on particle measurement by digital holography. , 2014, , .		0
248	Plasma-catalytic oxidation of diluted formaldehyde over Cu-Ce oxide catalysts. , 2015, , .		0
249	Plasma-Catalyst Coupling for Enhanced Oxidation of Ethyl Acetate Over V ₂ O ₅ /TiO ₂ Nanofiber Catalyst. , 2017, , .		0
250	Plasma-assisted adsorption of elemental mercury on CeO2/TiO2 at low temperatures. IOP Conference Series: Earth and Environmental Science, 2017, 94, 012050.	0.2	0
251	A real-time optimization method for economic and effective operation of electrostatic precipitators. Journal of the Air and Waste Management Association, 2020, 70, 708-720.	0.9	0
252	Pollutant Control by Electric Methods. Advanced Topics in Science and Technology in China, 2021, , 105-198.	0.0	0

#	Article	IF	CITATIONS
253	Pollutant Control by Absorption Methods. Advanced Topics in Science and Technology in China, 2021, , 199-279.	0.0	0
254	Pollutant Control by Catalytic Methods. Advanced Topics in Science and Technology in China, 2021, , 21-103.	0.0	0
255	The Study on the Active Site Regulated RuOx/Sn0.2Ti0.8O2 Catalysts with Different Ru Precursors for the Catalytic Oxidation of Dichloromethane. Catalysts, 2021, 11, 1306.	1.6	0
256	Effect of Dimethyl Formamide (DMF) on Vanadium Reloading Over V-Ti SCR Catalyst. Frontiers in Energy Research, 2022, 10, .	1.2	0